HHS Public Access

Author manuscript

Immunity. Author manuscript; available in PMC 2019 July 17.

Published in final edited form as:

Immunity. 2018 July 17; 49(1): 107–119.e4. doi:10.1016/j.immuni.2018.04.021.

TRPV4 Channel Signaling in Macrophages Promotes Gastrointestinal Motility via Direct Effects on Smooth Muscle Cells

Jialie Luo[1], **Aihua Qian**[2], **Landon K. Oetjen**[3], **Weihua Yu**[4], **Pu Yang**[1], **Jing Feng**[1], **Zili Xie**[1], **Shenbin Liu**[1], **Shijin Yin**[5], **Dari Dryn**[6,11], **Jizhong Cheng**[7], **Terrence E. Riehl**[8], **Alexander V. Zholos**[6], **William F. Stenson**[8], **Brian S. Kim**[1,3,9,10], and **Hongzhen Hu**[1,10,a]

[1]Center for the Study of Itch, Department of Anesthesiology, Washington University School of Medicine, St. Louis, MO 63110, USA

[2]Department of Gastroenterology, Ruijin Hospital, Shanghai Jiaotong University, Shanghai 200025, China

[3]Division of Dermatology, Department of Medicine, Washington University School of Medicine, St. Louis, MO 63110, USA

[4]Department of Anatomy, Chongqing Medical University, Chongqing 400016, China

[5]College of Pharmacy, South-Central University for Nationalities, Wuhan, Hubei 430073, China

[6]Department of Biophysics, Institute of Biology, Taras Shevchenko National University of Kyiv, Kyiv 03022, Ukraine

[7]Department of Medicine, Baylor College of Medicine, Houston 77030, TX, USA

[8]Division of Gastroenterology, Department of Medicine, Washington University School of Medicine, St. Louis, MO 63110, USA

[9]Department of Pathology and Immunology, Washington University School of Medicine, St. Louis, MO 63110, USA

Summary

[10]**Correspondence:** Hongzhen Hu, Ph.D., Associate Professor, Department of Anesthesiology, Center for the Study of Itch, Washington University School of Medicine in St. Louis, 660 South Euclid Avenue, St. Louis, MO 63110, hongzhen.hu@wustl.edu, Brian S. Kim, M.D., Assistant Professor, Division of Dermatology, Department of Medicine, Center for the Study of Itch, Washington University School of Medicine in St. Louis, 660 South Euclid Avenue, St. Louis, MO 63110, briankim@wustl.edu.

[11]Present address: Department of Cellular Membranology, A.A. Bogomoletz Institute of Physiology, National Academy of Sciences of Ukraine, Kyiv 01024, Ukraine

[a]Lead contact

Author Contributions

J.L. and H.H. contributed to all aspects of the manuscript (conceptual design, experimentation, and writing); J.L., A.Q., L.K.O., W.Y., P.Y., J.F., Z.X.; S.L., S.Y., D.D., J.C., T.E.R., and A.V.Z. contributed to experimentation; W.F.S. and B.S.K. contributed to writing the manuscript.

Declaration of Interests

The authors declare no competing interests.

Intestinal macrophages are critical for gastrointestinal (GI) homeostasis, but our understanding of their role in regulating intestinal motility is incomplete. Here, we report that CX3C chemokine receptor 1-expressing muscularis macrophages (MMs) were required to maintain normal GI motility. MMs expressed the transient receptor potential vanilloid 4 (TRPV4) channel, which senses thermal, mechanical, and chemical cues. Selective pharmacologic inhibition of TRPV4 or conditional deletion of TRPV4 from macrophages decreased intestinal motility and was sufficient to reverse the GI hypermotility that is associated with chemotherapy treatment. Mechanistically, stimulation of MMs via TRPV4 promoted the release of prostaglandin E2 and elicited colon contraction in a paracrine manner via prostaglandin E receptor signaling in intestinal smooth muscle cells without input from the enteric nervous system. Collectively, our data identify TRPV4-expressing MMs as an essential component required for maintaining normal GI motility and provide potential drug targets for GI motility disorders.

In brief

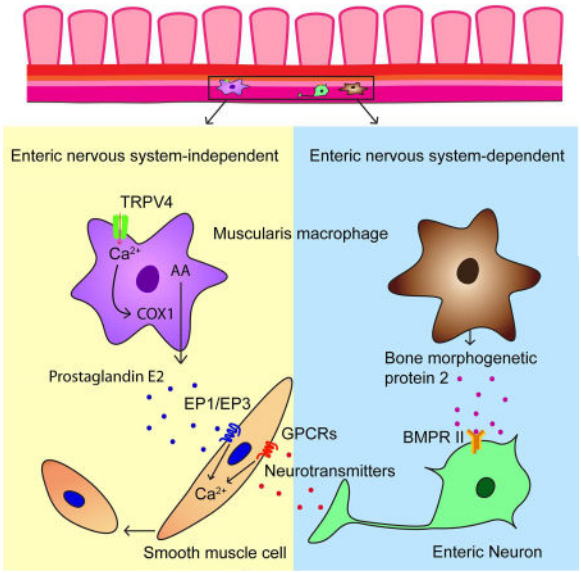

How intestinal macrophages regulate intestinal motility remains poorly understood. Luo et al. demonstrate that muscularis macrophages expressing the TRPV4 channel promote GI motility by directly affecting the function of intestinal smooth muscle cells independent of the enteric nervous system.

Introduction

Macrophages exhibit highly diverse properties and play critical roles in maintaining tissue homeostasis throughout the body (Glass and Natoli, 2016; Gordon and Taylor, 2005; Wynn et al., 2013). Additionally, they have been implicated in a variety of processes including, but not limited to, protection against infectious organisms, cancer, and unchecked inflammation (Brown et al., 2017; De Palma et al., 2017; Markel et al., 2007; Mowat et al., 2017; Zhao et al., 2008). Emerging studies indicate that macrophages have highly specialized functions that are likely shaped by the tissue microenvironment (Gosselin et al., 2017; Hulsmans et al.,

2017; Lavin et al., 2014; Nguyen et al., 2011; Okabe and Medzhitov, 2014; Paolicelli et al., 2011; Soncin et al., 2018; Theurl et al., 2016). In the gastrointestinal (GI) tract, macrophages derived from yolk sac embryonic precursors are not capable of self-maintenance but constantly replenished by monocytes derived from the bone marrow in adulthood (Bain et al., 2014; Ginhoux and Guilliams, 2016). The largest population of macrophages in the body reside within the GI tract with a high density in the lamina propria (LP) and the smooth muscle, or muscularis, layers of the colon (Lee et al., 1985). Although it is well known that LP macrophages play crucial roles in GI immunity to pathogens (Bain and Mowat, 2014; Grainger et al., 2017; Joeris et al., 2017), the functions of muscularis macrophages (MMs) in the smooth muscle layers are not well understood.

MMs have been shown to differentially influence GI motility in a multitude of settings including postoperative ileus (Boeckxstaens and de Jonge, 2009; Wehner et al., 2007), recovery of motility from surgery (Farro et al., 2017), diabetic gastroparesis (Choi et al., 2010), and enteric helminth infections (Zhao et al., 2008). Although MMs have been shown to interact with both the extrinsic autonomic nervous system and intrinsic enteric nervous system (ENS) to regulate GI motility (Gabanyi et al., 2016; Muller et al., 2014), the precise mechanisms that underlie these neuroimmune interactions remain poorly understood. Further, MMs have been shown to be in close proximity to smooth muscle cells (SMCs) in the muscularis layers (Bain and Mowat, 2014; De Schepper et al., 2017), provoking the hypothesis that direct macrophage-smooth muscle cell interactions may regulate GI motility.

GI dysmotility is one of the most common medical complaints and can present in a variety of settings ranging from irritable bowel syndrome (IBS) to side effects of chemotherapy that can impact life-saving therapy (Cash and Chey, 2005; McQuade et al., 2016). Chemotherapy-induced diarrhea is a common side effect that frequently causes patient morbidity and mortality and often results in dose reduction or cessation of therapy (McQuade et al., 2016; Stein et al., 2010). Therefore, understanding the precise mechanisms that underlie both physiological and pathological GI motility is of paramount importance.

Transient receptor potential (TRP) channels are a large superfamily of cation channels that regulate a number of sensory functions including vision, taste, thermosensation, pain, and itch (Damann et al., 2008; Luo et al., 2015; Ramsey et al., 2006; Venkatachalam and Montell, 2007). A subset of TRP channels are expressed in the gut and have been shown to regulate GI motility under both steady state and pathological conditions (Cenac et al., 2015; Tsvilovskyy et al., 2009; Wouters et al., 2016). TRPV4 specifically is a molecular sensor of thermal, mechanical, and chemical cues, which has been shown to be expressed in epithelial cells and neurons in the gut and contribute to both somatic and visceral hypersensitivity as well as GI inflammation (Cenac et al., 2015; D'Aldebert et al., 2011; Holzer, 2011; Nilius and Szallasi, 2014; Voets, 2014). However, whether TRPV4 regulates GI motility remains to be explored.

In this study, we demonstrated that CX3C chemokine receptor 1 (CX3CR1)-positive MMs expressed TRPV4 and identified a role for macrophage-specific TRPV4 expression in mediating colon motility. We uncovered a direct interaction between MMs and SMCs promoting colon contractility that was regulated by TRPV4 and commenced independently

of the ENS. Employing macrophage-specific deletion as well as pharmacologic inhibition of TRPV4, we were able to attenuate chemotherapy-associated GI dysmotility. Collectively, our findings indicate that TRPV4 may represent a therapeutic target for GI motility disorders and they highlight a paradigm in which macrophages directly influence smooth muscle physiology in the gut.

Results

TRPV4 promotes intestinal motility

Although several members of the TRP family are expressed in the gut and have been implicated in controlling GI motility, the specific contributions of TRPV4 to this process remain largely unknown. To explore the role of TRPV4 in motility, we measured GI transit by examining the distribution of an orally administered fluorescent dye along the GI tract over 90 min in both *Trpv4*$^{+/+}$ and *Trpv4*$^{-/-}$ mice (Shah et al., 2010). GI transit was significantly reduced in *Trpv4*$^{-/-}$ mice compared to control *Trpv4*$^{+/+}$ mice (Figure 1A). In further support of reduced GI motility, the number of formed fecal pellets retained in the colon was significantly increased in *Trpv4*$^{-/-}$ mice compared to *Trpv4*$^{+/+}$ mice (Figures 1B and 1C), while the water content of freshly expelled fecal pellets was significantly reduced in *Trpv4*$^{-/-}$ mice in comparison to *Trpv4*$^{+/+}$ mice (Figure 1D). Collectively, these results demonstrated that global loss of TRPV4 function disrupted normal GI motility in mice.

We next tested whether activation of TRPV4 directly increases GI motility *in vivo* by counting the total number of fecal pellets expelled within 30 min after intraperitoneal (i.p.) injection of GSK1016790A (GSK101), a potent and selective TRPV4 agonist (Thorneloe et al., 2008). GSK101 significantly increased the number of fecal pellets in *Trpv4*$^{+/+}$ mice (Figure 1E) but not *Trpv4*$^{-/-}$ mice (Figure 1F). In agreement with our *in vivo* studies, we found that GSK101 elicited robust contractile responses in *ex vivo* colon strips from *Trpv4*$^{+/+}$ mice in a concentration-dependent manner (Figures S1A and S1B), while colon strips from *Trpv4*$^{-/-}$ mice failed to respond (Figures 1G and 1H), indicating that the effect of GSK101 was highly specific. Further in support of this, GSK101-induced colon contraction in *Trpv4*$^{+/+}$ mice was abolished by two selective TRPV4 antagonists, HC067047 (HC067) (Everaerts et al., 2010) and GSK2193874 (GSK219) (Thorneloe et al., 2012) (Figures S1C and S1D). Combined, these studies established that selective activation of TRPV4 was sufficient to induce intestinal smooth muscle contraction *ex vivo* and regulated GI motility *in vivo* under homeostatic conditions.

To examine whether TRPV4 may also regulate gut motility in pathologic states, we employed a model of chemotherapy-associated GI dysmotility where mice were treated with the chemotherapy drug irinotecan (IRI). As in patients who receive IRI, we detected significantly accelerated GI transit in wild-type (*wt*) mice treated with IRI as measured by dye migration (Figure 1I). *Trpv4* mRNA levels were significantly increased in the colon of mice treated with IRI (Figure 1J), and both pharmacological inhibition (Figure 1K) and genetic ablation of TRPV4 (Figure 1L) significantly attenuated the increase in GI transit induced by IRI administration. Collectively, these studies demonstrated that TRPV4 played an important role in regulating homeostatic and pathological GI motility. However, the cellular mechanisms by which TRPV4 influences these processes remained unknown.

TRPV4 is functionally expressed by intestinal MMs

GI motility is traditionally believed to be dictated by synchronized activity from intestinal SMCs, pacemaker interstitial cells of Cajal (ICCs), and motor neurons in the ENS (Sanders et al., 2012). However, whether these cells express TRPV4 is not well defined. In previous studies, the expression pattern of TRPV4 has been investigated by Western blot and immunohistochemical methods using TRPV4 antibodies (D'Aldebert et al., 2011; Mochizuki et al., 2009), but the specificity of commonly used TRPV4 antibodies has been a recent area of controversy (Cenac et al., 2010; Grant et al., 2007; Ryskamp et al., 2011). To circumvent these potential technical difficulties, we used a transgenic approach to identify TRPV4-expressing cells by expressing eGFP under the control of the endogenous TRPV4 promoter (designated as *Trpv4*^{eGFP}) (Gong et al., 2003; Luo et al., 2018).

In order to identify TRPV4-eGFP^{+} cells in the colon, we undertook a rigorous analysis of the morphology and cell surface markers of TRPV4-eGFP^{+} cells. We found that the TRPV4-eGFP^{+} cells in the whole-mount preparations of the longitudinal muscle layer and the myenteric plexus displayed a macrophage-like morphology and expressed F4/80 and CD206, commonly used colonic macrophage markers (Mikkelsen, 2010) (Figures 2A–2C). Further, we did not detect any co-localization of TRPV4-eGFP with HuC/D (a pan-neuronal marker) (Hu et al., 2002), Anoctamin-1 (ANO1) (a marker for ICCs) (Gomez-Pinilla et al., 2009), Sox10 (a glial marker) (Boesmans et al., 2015), or alpha smooth muscle actin (α-SMA) (a specific marker for SMCs) in whole-mount preparations of the longitudinal muscle layer and the myenteric plexus from *Trpv4*^{eGFP} mice (Figures 2D–2G). To further characterize TRPV4-expressing cells, we isolated cells from the muscularis externa and performed flow cytometry. Nearly all of the TRPV4-eGFP^{+} CD45^{+} cells were CD11b^{+} and major histocompatibility complex (MHC) II^{+} (Figure 2H), consistent with a MM identity (Muller et al., 2014). In further support of their macrophage phenotype, these cells were also CD64^{+}, F4/80^{+}, CX3CR1^{+}, and CD206^{+} (Figure 2I). In contrast to infiltrating monocytes that highly express Ly6C, TRPV4-eGFP^{+} CD45^{+} cells lacked expression of Ly6C (Figure 2I), demonstrating that TRPV4 was expressed by a distinct subpopulation of resident MMs in mouse colon.

Next, we characterized the functional consequences of TRPV4 signaling in sort-purified MMs (Figures 3A and 3B). Application of the TRPV4 agonist GSK101 elicited a robust intracellular Ca^{2+} ($[Ca^{2+}]_i$) response in *Trpv4*$^{+/+}$ MMs, which was suppressed by the TRPV4 antagonist GSK219 (Figures 3C, 3D and 3F). As expected, GSK101 did not elicit measurable $[Ca^{2+}]_i$ response in the *Trpv4*$^{-/-}$ MMs (Figures 3E and 3F), although ATP elicited robust $[Ca^{2+}]_i$ responses in MMs from both *Trpv4*$^{+/+}$ and *Trpv4*$^{-/-}$ mice (Jacob et al., 2013). GSK101 also activated an outwardly rectifying TRPV4-like current in the TRPV4-eGFP^{+} MMs freshly isolated from the tunica muscularis externa of *Trpv4*^{eGFP} mice that was abolished by the TRPV4 antagonist HC067 (Figures 3G–3I). Thus, these studies demonstrated that MMs expressed functional TRPV4.

Consistent with a lack of TRPV4 expression in intestinal SMCs, GSK101 had no effect on membrane currents evoked in isolated mouse colonic SMCs, though carbachol evoked robust currents (Figures S2A and S2B). GSK101 also failed to elicit a $[Ca^{2+}]_i$ response in freshly isolated mouse colonic SMCs (Figures S2C and S2D). Similarly, application of GSK101 did

not evoke a measurable $[Ca^{2+}]_i$ response in cultured mouse colonic myenteric neurons (Figures S2E and S2F). Further, blocking enteric neurotransmission with tetrodotoxin (TTX) did not suppress the GSK101-elicited contractile response (Figure S3). Collectively, these results demonstrated that MMs, but not traditional components of intestinal contractile machinery, express functional TRPV4 and TRPV4-dependent colon contraction occurred independently of the ENS.

Optogenetic and chemogenetic stimulation of intestinal macrophages produces ENS-independent colon contraction

The selective expression of TRPV4 on MMs (Figure 2) and the ability of GSK101 to induce colonic contraction without ENS input (Figure S3) suggest that MM-specific stimulation was sufficient to induce colon contraction. To test this possibility, we sought to undertake an approach to explore gut motility by directly stimulating MMs using both optogenetic and chemogenetic methods with *Cx3cr1*^{CreER} line based on the finding that TRPV4-epressing MMs are CX3CR1^{hi} (Figure 2I). Thus, we first expressed the H134R variant of channelrhodopsin-2/YFP (ChR2) in macrophages by crossing *Cx3cr1*^{CreER} mice with *ChR2* mice to create *Cx3cr1*^{CreER}*;ChR2* mice, which enabled the direct stimulation of colonic MMs with blue light illumination. We confirmed the selective expression of ChR2-YFP in F4/80$^+$ MMs after tamoxifen treatment using immunofluorescent staining (Figures 4A and 4B). Further, optogenetic illumination with a 488 nm laser (blue light) evoked an inward current with a reversal potential around 0 mV in MMs sort-purified from Cre$^+$ but not Cre$^-$ *Cx3cr1*^{CreER}*;ChR2* mice (Figures 4C–4E). As expected, *ex vivo* illumination of isolated colon strips from Cre$^+$ but not Cre$^-$ *Cx3cr1*^{CreER}*;ChR2* mice produced contractile responses (Figure 4F). Treatment with the neuronal inhibitor TTX did not significantly reduce the contraction (Figure 4G), further supporting that macrophage-mediated colon contraction did not require ENS input. In a complementary fashion, we also generated *Cx3cr1*^{CreER}*;Gq-DREADD* mice in which we could selectively stimulate all CX3CR1$^+$ MMs in the colon strips by using the DREADD ligand clozapine-N-oxide (CNO) (Urban and Roth, 2015). In contrast to local optogenetic stimulation by blue light, this approach enabled the stimulation of DREADD-expressing MMs in the entire colon. CNO application to colon strips from Cre$^+$ *Cx3cr1*^{CreER}*;Gq-DREADD* mice evoked robust and TTX-insensitive colon contractions (Figures 4H and 4I). Together, these results demonstrated that stimulation of MMs could induce colon contraction without ENS activity. However, the downstream molecular mediators of TRPV4- induced MM-mediated colon contraction remained unknown.

Colon contraction caused by MM stimulation requires PGE2 and COX-1

Previous studies have shown that nitric oxide (NO) and prostaglandin E2 (PGE2) are two of the primary inflammatory mediators released by activated intestinal macrophages and broadly regulate GI motility (Mori et al., 2014; Stenson, 2007). Although NO mainly inhibits the contraction of intestinal SMCs, PGE2 has a complex effect on GI motility as it can both increase and reduce intestinal muscle tone via distinct membrane bound G protein-coupled E-prostanoid receptors (EP1–4) (Wang et al., 2005). Both EP1 and EP3 are involved in PGE2-induced contraction of isolated guinea pig ileal SMCs (Botella et al., 1993) as well as PGE2-elicited contraction of small intestine in rabbits (Grasa et al., 2006; Okada et al., 2000). Consistent with the stimulatory effect of EP1 and EP3 on intestinal motility,

application of PGE2 directly to freshly isolated colonic SMCs elicited a robust $[Ca^{2+}]_i$ response that was severely attenuated by EP1 receptor antagonist SC 51089 (SC510) and EP3 receptor antagonist L-798106 (L798) but not EP2 receptor antagonist PF 04418948 (PF044) and EP4 receptor antagonist L-161982 (L161) (Figure S4). Further, GSK101-elicited colon contraction was suppressed by EP1 receptor antagonist (Figure 5A) or EP3 receptor antagonist (Figure 5B) in a concentration-dependent manner, but not affected by high concentrations of either EP2 receptor antagonist or EP4 receptor antagonist (Figure S5A). Thus, these observations demonstrated that TRPV4 regulation of gut motility depended on EP1- and EP3-mediated PGE2 signaling.

PGE2 is a major metabolite of cyclooxygenase (COX), an enzyme that exists in at least two different isoforms (constitutively expressed COX-1 and inducible COX-2). To determine the role of COX-1 and COX-2 in TRPV4-mediated colon contraction, we measured the GSK101-induced colon contraction in both *Cox-1*$^{-/-}$ and *Cox-2*$^{-/-}$ mice. GSK101-induced colon contraction was severely attenuated in *Cox-1*$^{-/-}$ mice, but not *Cox-2*$^{-/-}$ mice compared to their *wt* littermates (Figures 5C and 5D). Further, SC 560, a selective COX-1 inhibitor, markedly suppressed GSK101-induced colon contraction (Figure S5B). Collectively, these studies showed that TRPV4-mediated colon contraction, in addition to being dependent on PGE2, was selectively dependent on COX-1, a key enzyme that generates PGE2.

To determine if TRPV4 signaling on MMs could elicit PGE2 release directly from these cells, we stimulated sort-purified MMs with GSK101 and measured PGE2 levels. GSK101 stimulation evoked nearly a four-fold increase of PGE2 release from MMs of *Trpv4*$^{+/+}$ mice compared to vehicle treatment. Increased PGE2 release was absent from GSK101-stimulated MMs harvested from *Trpv4*$^{-/-}$ mice (Figure 5E). Furthermore, GSK101-induced PGE2 release was completely abolished in a Ca^{2+}-free condition (Figure S5C), confirming that TRPV4-mediated Ca^{2+} influx was essential for increased PGE2 levels. Activation of other TRP channels including TRPA1 by allyl isothiocyanate (AITC) and TRPV1 by capsaicin did not evoke significant PGE2 release in MMs (Figure 5F), suggesting that selective activation of TRPV4 in MMs promoted PGE2 release. Consistent with our studies showing TRPV4-mediated colon contraction was COX-1 dependent, GSK101 did not evoke PGE2 release in MMs from *Cox-1*$^{-/-}$ mice (Figure S5D). Previous studies have shown that activation of extracellular signal-regulated kinase 1 and 2 (ERK1/2) activates phospholipase A2 (PLA2), leading to increased release of arachidonic acid, the substrate of PGE2 production catalyzed by COX-1 (Sauvant et al., 2002). Similar to these findings, both ERK1/2 (PD98059) and PLA2 (arachidonyl trifluoromethyl ketone, ATK) inhibitors markedly inhibited TRPV4-mediated PGE2 release from MMs (Figure 5G). In line with the involvement of PGE2 signaling in TRPV4-evoked MM-mediated colon contraction, we observed that both optogenetic and chemogenetic stimulations of MMs promoted PGE2 release and induced EP1 and EP3 receptor-dependent colon contraction (Figures 5H–5K). Collectively, these studies demonstrated that stimulation of MMs resulted in the production of mediators known to control gut motility and provoked the hypothesis that MM-specific expression of TRPV4 was a critical mediator of gut motility *in vivo*.

Macrophage-specific TRPV4 expression regulates GI motility

To clearly define the role of macrophage-specific TRPV4 in promoting GI motility *in vivo*, we generated TRPV4-floxed mice (*Trpv4*$^{f/f}$) (Figure 6A) and crossed them with *Cx3cr1*^{CreER} mice to generate inducible macrophage-specific TRPV4 knockout mice (*Cx3cr1*^{CreER}; *Trpv4*$^{f/f}$) based on the finding that CX3CR1-eGFP was exclusively expressed by CD206^{+} F4/80^{+} MMs in muscularis externa of *Cx3cr1*^{eGFP} mice (Medina-Contreras et al., 2011). TRPV4 expression was significantly reduced in MMs sort-purified from the colon of Cre^{+} *Cx3cr1*^{CreER}; *Trpv4*$^{f/f}$ mice after tamoxifen treatment (Figures 6B and 6C). Intestinal motility was significantly decreased in the macrophage-specific Cre^{+} *Cx3cr1*^{CreER}; *Trpv4*$^{f/f}$ mice as evidenced by reduced GI transit (Figure 6D), increased number of formed fecal pellets retained in the colon (Figures 6E and 6F), and decreased water content in the fecal pellets (Figure 6G). Further, increased fecal pellet expulsion (Figure 6H) and colon contraction (Figures 6I and 6J) induced by GSK101 were markedly reduced in Cre^{+} *Cx3cr1*^{CreER}; *Trpv4*$^{f/f}$ mice in comparison to Cre^{-} littermate control mice. Together, these findings demonstrated that macrophage-specific expression of TRPV4 regulated homeostatic GI motility.

To determine if TRPV4 in macrophages contributes to pathological GI hypermotility associated with chemotherapy, we treated Cre^{+} *Cx3cr1*^{CreER}; *Trpv4*$^{f/f}$ mice with vehicle or IRI. We found that the GI dysfunction induced by IRI was significantly attenuated in Cre^{+} *Cx3cr1*^{CreER}; *Trpv4*$^{f/f}$ mice (Figure 6K). Taken together, these results confirmed that the MM-specific expression of TRPV4 directly regulated the function of intestinal SMCs to control GI motility. Thus, this study established a paradigm of direct GI regulation by the immune system that represented a therapeutic target for GI motility disorders.

Discussion

GI motility is controlled by many factors including neurotransmitters within the ENS and CNS, GI hormones, and various immune factors (Greenwood-Van Meerveld et al., 2017; Holzer, 2007). However, in this study, we uncovered a pathway by which the TRP channel protein TRPV4 promoted GI motility in both health and disease by influencing the function of intestinal MMs. Moreover, we showed that TRPV4-responsive MMs mediated contractility by directly interacting with SMCs, independently of neuronal input. Finally, we demonstrated that MM-specific TRPV4 was critically required for both homeostatic gut physiology and pathological dysmotility. Collectively, the current study highlighted a paradigm in which, beyond neuronal hypersensitivity and barrier inflammation, TRPV4 played a uniquely important role in regulating mechanical functions of the gut in both health and disease.

In recent years, the expression of TRPV4 in the gut has been largely characterized by the use of polyclonal antibodies, the specificity of which has been controversial (Cenac et al., 2010; Grant et al., 2007; Ryskamp et al., 2011). Therefore, to avoid technical limitations, we sought to undertake an alternative genetic approach using *Trpv4*^{eGFP} reporter mice. Employing these mice, we have demonstrated that TRPV4 channels were selectively expressed *in vivo* by CX3CR1^{+} MMs but not present in other components of the contractile apparatus including ICCs, SMCs, and ENS. We found that loss of TRPV4 function was

sufficient to impair GI motility under steady-state conditions, suggesting that TRPV4 was a constitutively active signaling molecule evoked by warm temperature or endogenous ligands in the gut and critically required for GI homeostasis. In the setting of pathologic GI dysmotility, we found that both genetic deletion and pharmacologic inhibition of TRPV4 were sufficient to reverse dysmotility and that TRPV4 expressed specifically on MMs was required for this process. Collectively, these studies demonstrated roles for both TRPV4 and MMs in promoting both normal gut motility and pathological dysmotility. $CX3CR1^{+}$ LP macrophages are also present in the gut, but they are positioned away from the SMCs and are critically involved in GI immunity. However, in the absence of specific *in vivo* approaches whereby we can dissect the role of LP macrophages compared to MMs, we cannot rule out the possible effect of $CX3CR1^{+}$ LP macrophages in regulating GI motility. Nevertheless, MMs-mediated PGE2 release and the involvement of PGE2 signaling in macrophage-mediated colon contraction supported the critical role of MMs in regulating GI motility.

Previous studies have demonstrated that MMs secrete BMP2 to stimulate the ENS and influence gut motility, presumably by driving the output from excitatory enteric neurons (Ambudkar, 2009; Muller et al., 2014; Tsvilovskyy et al., 2009). However, our findings demonstrated an additional pathway by which MMs acted directly on SMCs to regulate colon contractility. Our current findings suggested that PGE2 acted as a paracrine factor derived from MMs to mediate mechanical contraction. Although we and others have shown that PGE2 can activate distinct types of myenteric neurons (Hu et al., 2003; Manning et al., 2002), we found that blocking enteric neurotransmission with TTX did not affect the contractile responses elicited by TRPV4 activation and MMs stimulated by pharmacologic, optogenetic, and chemogenetic approaches. One potential explanation for this discrepancy is that the amount of PGE2 released by stimulated MMs is enough to cause contraction of SMCs but may not be sufficient to elicit action potential firing in enteric neurons. Thus, by identifying the contributions of MMs to colon contractility through direct activity on SMCs, we have also discovered that PGE2 derived from MMs could act as key effector molecule of gut motility.

Previous studies have shown that PGE2 production catalyzed by COX-2 is a major inflammatory mediator contributing to the pathogenesis of decreased gut motility seen in post-operative ileus (Schwarz et al., 2001). Given that both COX-1 and COX-2 can lead to PGE2 production via distinct pathways, we further hypothesized that PGE2 might have heterogeneous physiological effects depending on the context. Indeed, downstream of PGE2, EP1/3 receptor signaling mediate intestinal contraction but EP2/4 receptors mediate relaxation. Although we could not exclude the possibility that induced expression of COX-2 contributes to TRPV4-mediated contractile responses in inflamed states, our data demonstrated that COX-1-derived PGE2 from MMs was the critical mediator of GI motility under steady state. Taken together, these findings demonstrated unique and highly specific regulatory mechanisms that likely underlay the regulation of GI motility by TRPV4-expressing MMs.

In summary, we have discovered a role for TRPV4 in promoting both homeostatic and pathological GI motility. We further demonstrated that TRPV4-expressing MMs critically

mediated GI contraction by directly influencing SMC function in the colon independently of contributions from the ENS. Thus, we have identified a direct macrophage-smooth muscle axis in GI motility. The observation that these mechanisms were highly specific to MMs has also uncovered a role for the COX-1-PGE2 pathway in gut physiology. The identification of these additional molecular and cellular targets in GI motility open the possibility for therapeutic approaches involving TRPV4 and MMs in the treatment of a wide variety of GI motility disorders.

STAR Methods

CONTACT FOR REAGENT AND RESOURCE SHARING

Further information and requests for resources and reagents should be directed to and will be fulfilled by the Lead Contact, Hongzhen Hu (hongzhen.hu@wustl.edu)

EXPERIMENTAL MODEL AND SUBJECT DETAILS

Mice—Adult (8–10 weeks) male and female C57BL/6J mice (Jackson Laboratories), *Trpv4*^{eGFP} (Mutant Mouse Regional Resource Centers, MMRRC), *Trpv4*$^{-/-}$ (Suzuki et al., 2003), *Cox1*$^{-/-}$ (Houchen et al., 2000), *Cox2*$^{-/-}$(Houchen et al., 2000), *Cx3cr1*^{CreER} (kindly provided by Gwen Randolph), *ChR2* (Jackson Laboratories), *Gq-DREADD* (Jackson Laboratories), and *Trpv4*$^{f/f}$ (Luo et al., 2018) mice were used for this study. All the experimental procedures were approved by the Institutional Animal Care and Use Committee of Washington University School of Medicine. All mice were randomly allocated to different experimental groups by the lab managers who were blinded to the experimental design. Tamoxifen induction of inducible Cre-driver lines was performed by intraperitoneal administration of tamoxifen for 5 consecutive days at 75 mg/kg in 0.2 mL of corn oil. Animals were used 7 days after the final tamoxifen administration.

METHOD DETAILS

Dissociation of myenteric neurons—Enzymatic dissociation was used to obtain myenteric neurons for live cell Ca^{2+} imaging as previously described (Hu et al., 2002). The myenteric plexus was dissected and divided into 0.5 cm segments that were then incubated in an enzyme cocktail containing per 100 ml Krebs solution, 125 mg collagenase type IA, 100 mg protease type IX, and 2.5 mg deoxyribonuclease I (DN-25; all from Sigma Biochemical Company). Incubation was at 37°C with continuous shaking for 35 min. The digest was then separated from the solution by centrifugation at 2,000 rpm for 10 min. The supernatant was discarded, and the pellets were washed with ice-cold Krebs solution and then recentrifuged twice. The cells were then plated on coverslips coated with poly-D-lysine. Culture medium was minimum essential medium containing: guinea pig serum (2.5%), L-glutamine (2 mM), penicillin (100 U/ml), streptomycin (100 μg/ml), and glucose (15 mM). The cultures were incubated at 37°C in a humidified atmosphere of 5% CO_2. Proliferation of non-neuronal cells was reduced by including cytosine arabinoside (10 μM) in the culture medium.

Isolation of intestinal SMCs—The longitudinal muscle layer was peeled off and placed in ice-cold modified Krebs solution containing (in mM): 120 NaCl, 12 glucose, 10 HEPES,

6 KCl, 2.5 $CaCl_2$, 1.2 $MgCl_2$ (pH 7.4 with NaOH). The tissue was cut into small pieces (1–2 mm length) and digested in 2 ml Ca^{2+}-free modified Krebs solution containing: collagenase (1 mg/ml), bovine serum albumin (1 mg/ml), and soybean trypsine inhibitor (1mg/ml) at 37°C for 16–17 min. After washing 2–3 times, the tissue pieces were slightly triturated with glass Pasteur pipette and kept in low-Ca^{2+} (0.8 mM) Krebs solution at 4°C until use.

Isolation of muscularis macrophages—Muscularis macrophages were isolated according to a previously described protocol (Ozaki et al., 2004). In brief, the colon was dissected out and washed several times with calcium- and magnesium-free (CMF) Hank's solution containing (in mM): 125 NaCl, 5.36 KCl, 15.5 $NaHCO_3$, 0.336 Na_2HPO_4, 10 glucose, 2.9 sucrose, and 11 HEPES. The colon was cut open alone the mesenteric border, pinned out in a Sylgard-lined dish, and washed with CMF Hank's solution. The smooth muscle layer was isolated by removing the mucosal and submucosal layers and cut into small pieces of 2–3 mm in length. The tissue pieces were incubated in 1.5 ml CMF Hank's solution for 30 min and then in a solution containing 15 mg/ml collagenase type II (300 U/mg, Worthington), 20 mg/ml soybean trypsin inhibitor (Worthington), and 20 mg/ml bovine serum albumin (Sigma) for 30 min at 37°C. After incubation, the tissue pieces were spun down, washed with CMF Hank's solution, and agitated with a pipette. Dispersed cells were filtered with 40 μm cell strainer and maintained in DMEM containing 10% FBS, 100 U/ml penicillin, and 100 μg/ml streptomycin.

Water content of fecal pellets—The freshly expelled fecal pellets were weighed and then reweighed after drying in an oven. Water content of the feces was calculated by the following formula: Water content % = (wet weight of the feces (mg) − dried weight of the feces (mg))/wet weight of the feces (mg) × 100.

IRI administration and GI transit measurement—For IRI administration, mice received an intraperitoneal injection of IRI (100 mg/kg) or vehicle control (1% DMSO +0.1% Tween 80). The intestinal transit was assayed 2 days later. For GI transit measurement, each mouse was injected with 100 μl FITC-Dextran (5 mg/ml) by oral gavage and sacrificed 90 min later. The whole gut was removed, and the small intestine and colon were equally divided into 10 and 3 segments, respectively. The contents in the stomach (Segment #1), small intestine segments (Segments #2–#11), cecum (Segment #12), and colon segments (Segments #13–#15) were flushed with 1 ml HBSS and centrifuged at 12,000g for 5 min. The fluorescence intensity of the supernatant was measured at 494 nm (absorption) / 521 nm (emission) wavelength. The geometric center (GC) was calculated with the formula: GC = Σ (% of total fluorescent signal per segment × segment number) / 100.

Isometric tension recording of intestinal strips—Intestinal contractile activity was determined as previously described (Gao et al., 2012). Briefly, 1 cm whole thickness strips from ileum or colon of each animal were mounted in the longitudinal direction in duplicate in 25 ml organ baths filled with Krebs-Ringer solution aerated with 5% CO_2 95% O_2 gas. The isometric force was monitored by an external force displacement transducer (World Precision Instruments, Inc.) connected to a PowerLab data acquisition system (AD

Instruments). The area under the curve (AUC) was calculated and expressed as the motility index. Testing chemicals were added into the recording chamber directly. For optogenetic stimulation, blue laser light generated with a diode-pumped crystal laser (CrystaLaser Model CL-473-050, Reno, NV) was delivered via an optical fiber, which was located to the proximity of the colon wall in the organ bath chamber.

PGE2 measurement—Muscularis macrophages were collected from *wt, Trpv4*$^{-/-}$, *Cox1*$^{-/-}$, *Cx3cr1*^{CreER}*;ChR2,* or *Cx3cr1*^{CreER}*;Gq-DREADD* mice and seeded in 24-well plates. Cells were stimulated with GSK101 in the absence or presence of extracellular Ca^{2+}, PD98059, or ATK for 10 min or by blue light, capsaicin, AITC, or CNO for 10 min. The level of PGE2 in the supernatant was measured using a prostaglandin E2 EIA kit according to manufacturer's instructions (Cayman).

Flow cytometry and cell sorting—Isolated MMs were stained with antibody cocktails on ice in the dark for 30 min. Antibody cocktails included antibodies against mouse CD45, CD11b, CD11c, MHC II, Ly6C, CD64, F4/80, CX3CR1, and CD206. Flow cytometry data were acquired on a LSRFortessa X20 (BD Biosciences) flow cytometer and analyzed using FlowJo 10 (Tree Star). Cell sorting was performed on a FACSAria II (BD Biosciences) cell sorter.

Immunofluorescence—Immunofluorescent staining of whole mounts was performed as described previously described (Gao et al., 2012). All preparations were examined with Nikon C1 Confocal Laser Microscope System equipped with NIS-Elements software. The primary antibodies included Rat anti-F4/80 (Biolegend), Rat anti-CD206 (AbDSerotec), Chicken anti-GFP (Aves Labs), Mouse anti-HuC/D (Invitrogen), Rabbit anti-Sox10 (Abcam), Rabbit anti-α-SMA (Novus), and Rabbit anti-ANO1 (Abcam). The secondary antibodies included Donkey anti-rat Cy3, Donkey anti-rabbit Cy3, Donkey anti-mouse Cy3, and Alexa Fluor 488 Donkey anti-chicken IgG.

Ca^{2+} imaging—Fura-2-based ratiometric measurement of $[Ca^{2+}]_i$ in myenteric neurons, intestinal macrophages, and SMCs was performed as previously described (Yin et al., 2013). Fluorescence at 340 and 380 nm excitation wavelengths was recorded using NIS-Elements imaging software. Values were averaged from about 100 cells in time-lapse images from each coverslip. Threshold of activation was defined as 3 standard deviations above the average (~20% above the baseline).

Whole-cell patch-clamp recording—Whole-cell patch-clamp recordings were performed using an EPC10 amplifier (HEKA Elektronik) at 25°C as previously described (Yin et al., 2013). Currents were filtered at 2 kHz and digitized at 10 kHz. Data were acquired using Patchmaster (HEKA Elektronik) and analyzed using Clampfit 10 (Molecular Devices).

RT-PCR—Total RNA was extracted using Trizol reagent (Invitrogen) according to the manufacturer's instructions. RNA was treated with DNase I (Invitrogen) and the cDNA was synthesized *in vitro* using ThermoScript® RT-PCR System kit (Invitrogen). The sequences of the primers were: mTRPV4 forward: 5'-CCTGCTGGTCACCTACATCA-3', reverse: 5'-

CTCAGGAACACAGGGAAGGA-3'; mGAPDH forward: 5'-GCACAGTCAAGGCCGAGAAT-3', reverse: 5'- GCCTTCTCCATGGTGGTGAA-3'. For the real-time RT-PCR detection of TRPV4 mRNA transcripts in the *Cx3cr1*^{CreER};*Trpv4*$^{f/f}$ and *wt* mice, the primers are: mTRPV4: 5'-TGCTTCTCAAGTGTTCACGCCTCTT-3', reverse: 5'-ATGTGCTGAAAGACCCCGATCTT-3'.

QUANTIFICATION AND STATISTICAL ANALYSIS

Values are reported as the mean ± standard error of the mean (SEM). Where means of two groups were compared, the 2-tailed Student's t-test was used to determine significance. Where multiple treatment groups or genotypes were compared, significance between means was calculated using one-way ANOVA with Tukey's post hoc test to calculate p values. A p value < 0.05 was considered statistically significant.

Supplementary Material

Refer to Web version on PubMed Central for supplementary material.

Acknowledgments

We thank Drs. M. Suzuki and A. Mizuno for providing TRPV4 KO mice, and Drs. Zhou-Feng Chen and Gwen Randolph for sharing breeder pairs of mice. We would also like to thank Lenard Lichtenberger, Qingyun Liu, Richard Breyer, Richard Clark, Edgar Walters, and Carmen Dessauer for constructive discussions. This work was supported, in whole or in part, by grants from the National Institutes of Health R01GM101218 and R01DK103901, Washington University DDRCC (NIDDK P30 DK052574), and Center for the Study of Itch of the Department of Anesthesiology of Washington University School of Medicine to H.H., and K08AR065577 and R01AR070116 to B.S.K.

References

Ambudkar IS. Unraveling smooth muscle contraction: the TRP link. Gastroenterology. 2009; 137:1211–1214. [PubMed: 19717126]

Bain CC, Bravo-Blas A, Scott CL, Gomez Perdiguero E, Geissmann F, Henri S, et al. Constant replenishment from circulating monocytes maintains the macrophage pool in the intestine of adult mice. Nat Immunol. 2014; 15:929–937. [PubMed: 25151491]

Bain CC, Mowat AM. Macrophages in intestinal homeostasis and inflammation. Immunol Rev. 2014; 260:102–117. [PubMed: 24942685]

Boeckxstaens GE, de Jonge WJ. Neuroimmune mechanisms in postoperative ileus. Gut. 2009; 58:1300–1311. [PubMed: 19671558]

Boesmans W, Lasrado R, Vanden Berghe P, Pachnis V. Heterogeneity and phenotypic plasticity of glial cells in the mammalian enteric nervous system. Glia. 2015; 63:229–241. [PubMed: 25161129]

Botella A, Delvaux M, Fioramonti J, Frexinos J, Bueno L. Stimulatory (EP1 and EP3) and inhibitory (EP2) prostaglandin E2 receptors in isolated ileal smooth muscle cells. Eur J Pharmacol. 1993; 237:131–137. [PubMed: 7689467]

Brown JM, Recht L, Strober S. The Promise of Targeting Macrophages in Cancer Therapy. Clin Cancer Res. 2017; 23:3241–3250. [PubMed: 28341752]

Cash BD, Chey WD. Diagnosis of irritable bowel syndrome. Gastroenterol Clin North Am. 2005; 34:205–220. [PubMed: 15862930]

Cenac N, Altier C, Motta JP, d'Aldebert E, Galeano S, Zamponi GW, et al. Potentiation of TRPV4 signalling by histamine and serotonin: an important mechanism for visceral hypersensitivity. Gut. 2010; 59:481–488. [PubMed: 20332520]

Cenac N, Bautzova T, Le Faouder P, Veldhuis NA, Poole DP, Rolland C, et al. Quantification and Potential Functions of Endogenous Agonists of Transient Receptor Potential Channels in Patients With Irritable Bowel Syndrome. Gastroenterology. 2015; 149:433–444. [PubMed: 25911511]

Choi KM, Kashyap PC, Dutta N, Stoltz GJ, Ordog T, Shea Donohue T, et al. CD206-positive M2 macrophages that express heme oxygenase-1 protect against diabetic gastroparesis in mice. Gastroenterology. 2010; 138:2399–2409. [PubMed: 20178793]

D'Aldebert E, Cenac N, Rousset P, Martin L, Rolland C, Chapman K, et al. Transient receptor potential vanilloid 4 activated inflammatory signals by intestinal epithelial cells and colitis in mice. Gastroenterology. 2011; 140:275–285. [PubMed: 20888819]

Damann N, Voets T, Nilius B. TRPs in our senses. Curr Biol. 2008; 18:R880–889. [PubMed: 18812089]

De Palma M, Biziato D, Petrova TV. Microenvironmental regulation of tumour angiogenesis. Nat Rev Cancer. 2017; 17:457–474. [PubMed: 28706266]

De Schepper S, Stakenborg N, Matteoli G, Verheijden S, Boeckxstaens GE. Muscularis macrophages: Key players in intestinal homeostasis and disease. Cell Immunol. 2017 Dec 26. 2017. doi: 10.1016/j.cellimm.2017.12.009

Everaerts W, Zhen X, Ghosh D, Vriens J, Gevaert T, Gilbert JP, et al. Inhibition of the cation channel TRPV4 improves bladder function in mice and rats with cyclophosphamide-induced cystitis. Proc Natl Acad Sci U S A. 2010; 107:19084–19089. [PubMed: 20956320]

Farro G, Stakenborg M, Gomez-Pinilla PJ, Labeeuw E, Goverse G, Giovangiulio MD, et al. CCR2-dependent monocyte-derived macrophages resolve inflammation and restore gut motility in postoperative ileus. Gut. 2017; 66:2098–2109. [PubMed: 28615302]

Gabanyi I, Muller PA, Feighery L, Oliveira TY, Costa-Pinto FA, Mucida D. Neuro-immune Interactions Drive Tissue Programming in Intestinal Macrophages. Cell. 2016; 164:378–391. [PubMed: 26777404]

Gao N, Luo J, Uray K, Qian A, Yin S, Wang G, et al. CaMKII is essential for the function of the enteric nervous system. PLoS One. 2012; 7:e44426. [PubMed: 22952977]

Ginhoux F, Guilliams M. Tissue-Resident Macrophage Ontogeny and Homeostasis. Immunity. 2016; 44:439–449. [PubMed: 26982352]

Glass CK, Natoli G. Molecular control of activation and priming in macrophages. Nat Immunol. 2016; 17:26–33. [PubMed: 26681459]

Gomez-Pinilla PJ, Gibbons SJ, Bardsley MR, Lorincz A, Pozo MJ, Pasricha PJ, et al. Ano1 is a selective marker of interstitial cells of Cajal in the human and mouse gastrointestinal tract. Am J Physiol Gastrointest Liver Physiol. 2009; 296:G1370–1381. [PubMed: 19372102]

Gong S, Zheng C, Doughty ML, Losos K, Didkovsky N, Schambra UB, et al. A gene expression atlas of the central nervous system based on bacterial artificial chromosomes. Nature. 2003; 425:917–925. [PubMed: 14586460]

Gordon S, Taylor PR. Monocyte and macrophage heterogeneity. Nat Rev Immunol. 2005; 5:953–964. [PubMed: 16322748]

Gosselin D, Skola D, Coufal NG, Holtman IR, Schlachetzki JCM, Sajti E, et al. An environment-dependent transcriptional network specifies human microglia identity. Science. 2017 Jun 23. 2017. doi: 10.1126/science.aal3222

Grainger JR, Konkel JE, Zangerle-Murray T, Shaw TN. Macrophages in gastrointestinal homeostasis and inflammation. Pflugers Arch. 2017; 469:527–539. [PubMed: 28283748]

Grant AD, Cottrell GS, Amadesi S, Trevisani M, Nicoletti P, Materazzi S, et al. Protease-activated receptor 2 sensitizes the transient receptor potential vanilloid 4 ion channel to cause mechanical hyperalgesia in mice. J Physiol. 2007; 578:715–733. [PubMed: 17124270]

Grasa L, Arruebo MP, Plaza MA, Murillo MD. PGE(2) receptors and their intracellular mechanisms in rabbit small intestine. Prostaglandins Other Lipid Mediat. 2006; 79:206–217. [PubMed: 16647635]

Greenwood-Van Meerveld B, Johnson AC, Grundy D. Gastrointestinal Physiology and Function. Handb Exp Pharmacol. 2017; 239:1–16. [PubMed: 28176047]

Holzer P. Role of visceral afferent neurons in mucosal inflammation and defense. Curr Opin Pharmacol. 2007; 7:563–569. [PubMed: 18029228]

Holzer P. Transient receptor potential (TRP) channels as drug targets for diseases of the digestive system. Pharmacol Ther. 2011; 131:142–170. [PubMed: 21420431]

Houchen CW, Stenson WF, Cohn SM. Disruption of cyclooxygenase-1 gene results in an impaired response to radiation injury. Am J Physiol Gastrointest Liver Physiol. 2000; 279:G858–865. [PubMed: 11052981]

Hu HZ, Gao N, Lin Z, Gao C, Liu S, Ren J, et al. Chemical coding and electrophysiology of enteric neurons expressing neurofilament 145 in guinea pig gastrointestinal tract. J Comp Neurol. 2002; 442:189–203. [PubMed: 11774335]

Hu HZ, Liu S, Gao N, Xia Y, Mostafa R, Ren J, et al. Actions of bradykinin on electrical and synaptic behavior of neurones in the myenteric plexus of guinea-pig small intestine. Br J Pharmacol. 2003; 138:1221–1232. [PubMed: 12711622]

Hulsmans M, Clauss S, Xiao L, Aguirre AD, King KR, Hanley A, et al. Macrophages Facilitate Electrical Conduction in the Heart. Cell. 2017; 169:510–522. [PubMed: 28431249]

Jacob F, Perez Novo C, Bachert C, Van Crombruggen K. Purinergic signaling in inflammatory cells: P2 receptor expression, functional effects, and modulation of inflammatory responses. Purinergic Signal. 2013; 9:285–306. [PubMed: 23404828]

Joeris T, Muller-Luda K, Agace WW, Mowat AM. Diversity and functions of intestinal mononuclear phagocytes. Mucosal Immunol. 2017; 10:845–864. [PubMed: 28378807]

Lavin Y, Winter D, Blecher-Gonen R, David E, Keren-Shaul H, Merad M, et al. Tissue-resident macrophage enhancer landscapes are shaped by the local microenvironment. Cell. 2014; 159:1312–1326. [PubMed: 25480296]

Lee SH, Starkey PM, Gordon S. Quantitative analysis of total macrophage content in adult mouse tissues. Immunochemical studies with monoclonal antibody F4/80. J Exp Med. 1985; 161:475–489. [PubMed: 3973536]

Luo J, Feng J, Liu S, Walters ET, Hu H. Molecular and cellular mechanisms that initiate pain and itch. Cell Mol Life Sci. 2015; 72:3201–3223. [PubMed: 25894692]

Luo J, Feng J, Yu G, Yang P, Mack MR, Du J, et al. Transient receptor potential vanilloid 4-expressing macrophages and keratinocytes contribute differentially to allergic and nonallergic chronic itch. J Allergy Clin Immunol. 2018; 141:608–619. [PubMed: 28807414]

Manning BP, Sharkey KA, Mawe GM. Effects of PGE2 in guinea pig colonic myenteric ganglia. Am J Physiol Gastrointest Liver Physiol. 2002; 283:G1388–1397. [PubMed: 12388206]

Markel TA, Crisostomo PR, Wang M, Herring CM, Meldrum KK, Lillemoe KD, et al. The struggle for iron: gastrointestinal microbes modulate the host immune response during infection. J Leukoc Biol. 2007; 81:393–400. [PubMed: 17255516]

McQuade RM, Stojanovska V, Donald E, Abalo R, Bornstein JC, Nurgali K. Gastrointestinal dysfunction and enteric neurotoxicity following treatment with anticancer chemotherapeutic agent 5-fluorouracil. Neurogastroenterol Motil. 2016; 28:1861–1875. [PubMed: 27353132]

Medina-Contreras O, Geem D, Laur O, Williams IR, Lira SA, Nusrat A, et al. CX3CR1 regulates intestinal macrophage homeostasis, bacterial translocation, and colitogenic Th17 responses in mice. J Clin Invest. 2011; 121:4787–4795. [PubMed: 22045567]

Mikkelsen HB. Interstitial cells of Cajal, macrophages and mast cells in the gut musculature: morphology, distribution, spatial and possible functional interactions. J Cell Mol Med. 2010; 14:818–832. [PubMed: 20132411]

Mochizuki T, Sokabe T, Araki I, Fujishita K, Shibasaki K, Uchida K, et al. The TRPV4 cation channel mediates stretch-evoked Ca2+ influx and ATP release in primary urothelial cell cultures. J Biol Chem. 2009; 284:21257–21264. [PubMed: 19531473]

Mori D, Watanabe N, Kaminuma O, Murata T, Hiroi T, Ozaki H, et al. IL-17A induces hypo-contraction of intestinal smooth muscle via induction of iNOS in muscularis macrophages. J Pharmacol Sci. 2014; 125:394–405. [PubMed: 25069526]

Mowat AM, Scott CL, Bain CC. Barrier-tissue macrophages: functional adaptation to environmental challenges. Nat Med. 2017; 23:1258–1270. [PubMed: 29117177]

Muller PA, Koscso B, Rajani GM, Stevanovic K, Berres ML, Hashimoto D, et al. Crosstalk between muscularis macrophages and enteric neurons regulates gastrointestinal motility. Cell. 2014; 158:300–313. [PubMed: 25036630]

Nguyen KD, Qiu YF, Cui XJ, Goh YPS, Mwangi J, David T, et al. Alternatively activated macrophages produce catecholamines to sustain adaptive thermogenesis. Nature. 2011; 480:104–U272. [PubMed: 22101429]

Nilius B, Szallasi A. Transient receptor potential channels as drug targets: from the science of basic research to the art of medicine. Pharmacol Rev. 2014; 66:676–814. [PubMed: 24951385]

Okabe Y, Medzhitov R. Tissue-specific signals control reversible program of localization and functional polarization of macrophages. Cell. 2014; 157:832–844. [PubMed: 24792964]

Okada Y, Hara A, Ma H, Xiao CY, Takahata O, Kohgo Y, et al. Characterization of prostanoid receptors mediating contraction of the gastric fundus and ileum: studies using mice deficient in prostanoid receptors. Br J Pharmacol. 2000; 131:745–755. [PubMed: 11030724]

Ozaki H, Kawai T, Shuttleworth CW, Won KJ, Suzuki T, Sato K, et al. Isolation and characterization of resident macrophages from the smooth muscle layers of murine small intestine. Neurogastroenterol Motil. 2004; 16:39–51.

Paolicelli RC, Bolasco G, Pagani F, Maggi L, Scianni M, Panzanelli P, et al. Synaptic Pruning by Microglia Is Necessary for Normal Brain Development. Science. 2011; 333:1456–1458. [PubMed: 21778362]

Ramsey IS, Delling M, Clapham DE. An introduction to TRP channels. Annu Rev Physiol. 2006; 68:619–647. [PubMed: 16460286]

Ryskamp DA, Witkovsky P, Barabas P, Huang W, Koehler C, Akimov NP, et al. The polymodal ion channel transient receptor potential vanilloid 4 modulates calcium flux, spiking rate, and apoptosis of mouse retinal ganglion cells. J Neurosci. 2011; 31:7089–7101. [PubMed: 21562271]

Sanders KM, Koh SD, Ro S, Ward SM. Regulation of gastrointestinal motility--insights from smooth muscle biology. Nat Rev Gastroenterol Hepatol. 2012; 9:633–645. [PubMed: 22965426]

Sauvant C, Holzinger H, Gekle M. Short-term regulation of basolateral organic anion uptake in proximal tubular OK cells: EGF acts via MAPK, PLA(2), and COX1. J Am Soc Nephrol. 2002; 13:1981–1991. [PubMed: 12138128]

Schwarz NT, Kalff JC, Turler A, Engel BM, Watkins SC, Billiar TR, et al. Prostanoid production via COX-2 as a causative mechanism of rodent postoperative ileus. Gastroenterology. 2001; 121:1354–1371. [PubMed: 11729115]

Shah SK, Moore-Olufemi SD, Uray KS, Jimenez F, Walker PA, Xue H, et al. A murine model for the study of edema induced intestinal contractile dysfunction. Neurogastroenterol Motil. 2010; 22:1132–e1290. [PubMed: 20591104]

Soncin I, Sheng J, Chen Q, Foo S, Duan K, Lum J, et al. The tumour microenvironment creates a niche for the self-renewal of tumour-promoting macrophages in colon adenoma. Nat Commun. 2018; 9:582. [PubMed: 29422500]

Stein A, Voigt W, Jordan K. Chemotherapy-induced diarrhea: pathophysiology, frequency and guideline-based management. Ther Adv Med Oncol. 2010; 2:51–63. [PubMed: 21789126]

Stenson WF. Prostaglandins and epithelial response to injury. Curr Opin Gastroenterol. 2007; 23:107–110. [PubMed: 17268236]

Suzuki M, Mizuno A, Kodaira K, Imai M. Impaired pressure sensation in mice lacking TRPV4. J Biol Chem. 2003; 278:22664–22668. [PubMed: 12692122]

Theurl I, Hilgendorf I, Nairz M, Tymoszuk P, Haschka D, Asshoff M, et al. On-demand erythrocyte disposal and iron recycling requires transient macrophages in the liver. Nat Med. 2016; 22:945–951. [PubMed: 27428900]

Thorneloe KS, Cheung M, Bao W, Alsaid H, Lenhard S, Jian MY, et al. An orally active TRPV4 channel blocker prevents and resolves pulmonary edema induced by heart failure. Sci Transl Med. 2012; 4:159ra148.

Thorneloe KS, Sulpizio AC, Lin Z, Figueroa DJ, Clouse AK, McCafferty GP, et al. N-((1S)-1-{[4-((2S)-2-{[(2,4-dichlorophenyl)sulfonyl]amino}-3-hydroxypropanoyl)-1-piperazinyl]carbonyl}-3-methylbutyl)-1-benzothiophene-2-carboxamide (GSK1016790A), a novel and potent transient receptor potential vanilloid 4 channel agonist induces urinary bladder contraction and hyperactivity: Part I. J Pharmacol Exp Ther. 2008; 326:432–442. [PubMed: 18499743]

Tsvilovskyy VV, Zholos AV, Aberle T, Philipp SE, Dietrich A, Zhu MX, et al. Deletion of TRPC4 and TRPC6 in mice impairs smooth muscle contraction and intestinal motility in vivo. Gastroenterology. 2009; 137:1415–1424. [PubMed: 19549525]

Urban DJ, Roth BL. DREADDs (designer receptors exclusively activated by designer drugs): chemogenetic tools with therapeutic utility. Annu Rev Pharmacol Toxicol. 2015; 55:399–417. [PubMed: 25292433]

Venkatachalam K, Montell C. TRP channels. Annu Rev Biochem. 2007; 76:387–417. [PubMed: 17579562]

Voets T. TRP Channels and Thermosensation. Handb Exp Pharmacol. 2014; 223:729–741. [PubMed: 24961967]

Wang D, Mann JR, DuBois RN. The role of prostaglandins and other eicosanoids in the gastrointestinal tract. Gastroenterology. 2005; 128:1445–1461. [PubMed: 15887126]

Wehner S, Behrendt FF, Lyutenski BN, Lysson M, Bauer AJ, Hirner A, et al. Inhibition of macrophage function prevents intestinal inflammation and postoperative ileus in rodents. Gut. 2007; 56:176–185. [PubMed: 16809419]

Wouters MM, Balemans D, Van Wanrooy S, Dooley J, Cibert-Goton V, Alpizar YA, et al. Histamine Receptor H1-Mediated Sensitization of TRPV1 Mediates Visceral Hypersensitivity and Symptoms in Patients With Irritable Bowel Syndrome. Gastroenterology. 2016; 150:875–887. [PubMed: 26752109]

Wynn TA, Chawla A, Pollard JW. Macrophage biology in development, homeostasis and disease. Nature. 2013; 496:445–455. [PubMed: 23619691]

Yin S, Luo J, Qian A, Du J, Yang Q, Zhou S, et al. Retinoids activate the irritant receptor TRPV1 and produce sensory hypersensitivity. J Clin Invest. 2013; 123:3941–3951. [PubMed: 23925292]

Zhao A, Urban JF Jr, Anthony RM, Sun R, Stiltz J, van Rooijen N, et al. Th2 cytokine-induced alterations in intestinal smooth muscle function depend on alternatively activated macrophages. Gastroenterology. 2008; 135:217–225. [PubMed: 18471439]

Highlights

1. Macrophage-specific *Trpv4*-deficient mice display reduced gastrointestinal motility.
2. Direct interactions between MMs and smooth muscle cells produce colon contraction.
3. Enteric nervous system is not involved in macrophage-mediated colon contraction.
4. TRPV4 inhibition reverses GI hypermotility associated with chemotherapy treatment.

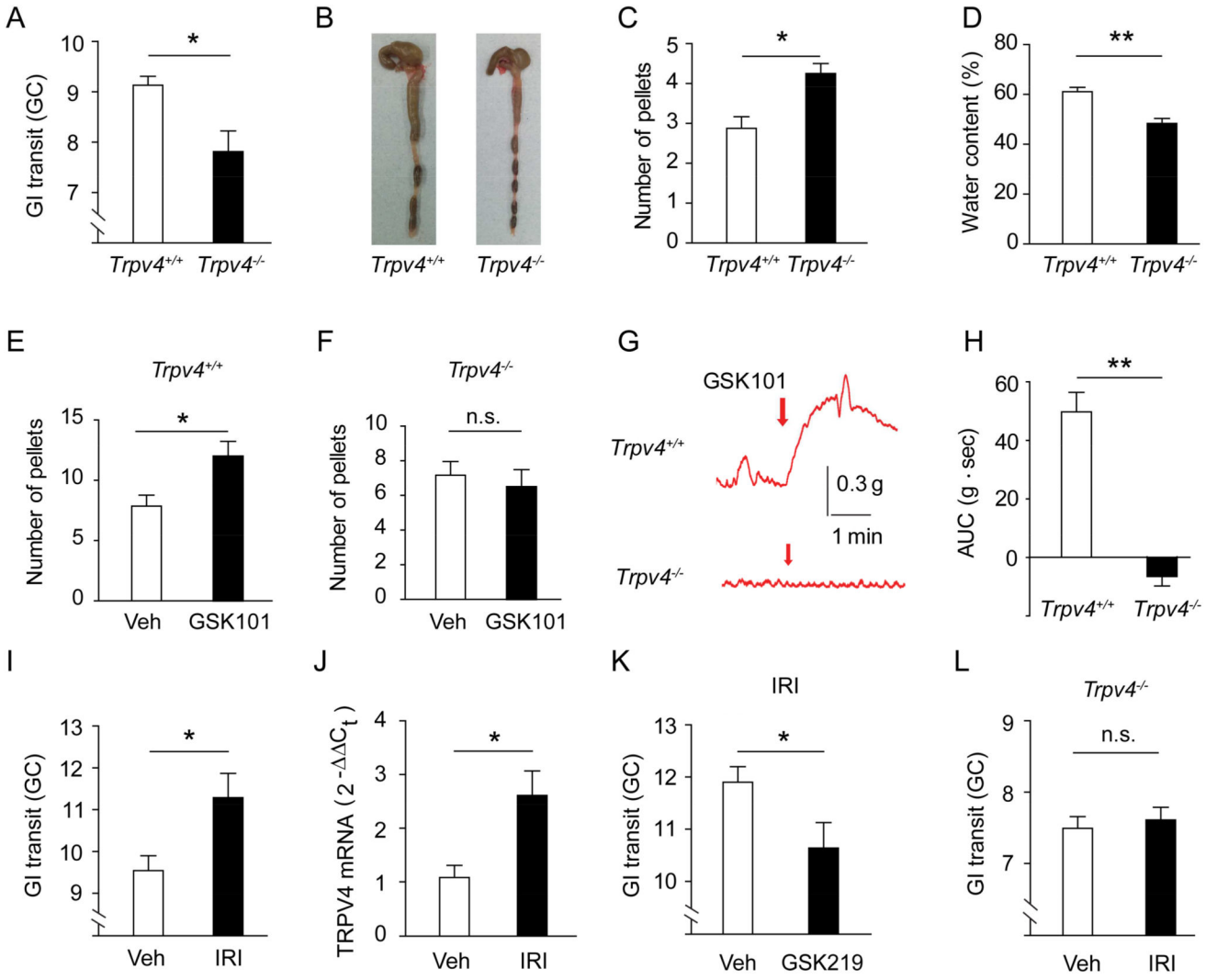

Figure 1. TRPV4 regulates GI motility under normal and pathological conditions

(A) GI transit measured by the geometric center of distribution (GC) of FITC–labeled dextran in *Trpv4*$^{+/+}$ and *Trpv4*$^{-/-}$ mice. n=6 mice per group.

(B–C) Representative images (B) and quantification (C) of formed fecal pellets retained in the colon of *Trpv4*$^{+/+}$ and *Trpv4*$^{-/-}$ mice. n=6 mice per group.

(D) Water content of fecal pellets from *Trpv4*$^{+/+}$ and *Trpv4*$^{-/-}$ mice. n=7 mice per group.

(E–F) The total number of fecal pellets expelled within 30 min after i.p. injections of vehicle (saline) or GSK101 (100 μg/kg) in *Trpv4*$^{+/+}$ (E) and *Trpv4*$^{-/-}$ (F) mice. n=6 mice per group.

(G–H) Representative traces (G) and quantification (H) of GSK101 (0.3 μM)-induced contractile responses in colon strips from *Trpv4*$^{+/+}$ and *Trpv4*$^{-/-}$ mice. n=16 segments from 4 mice per group.

(I) GI transit in *wt* mice after administration of vehicle or IRI (100 mg/kg). n=6 mice per group.

(J) TRPV4 mRNA expression in the colon of *wt* mice treated with vehicle or IRI. n=5 mice per group.

(K) GI transit in IRI-treated *wt* mice co-treated with vehicle or the TRPV4 inhibitor GSK219 (10 mg/kg). n=5 mice per group.
(L) GI transit in *Trpv4*$^{-/-}$ mice after administration of vehicle or IRI. n=5 mice per group.
All data are pooled from two to four independent experiments. Data are mean ± SEM. In this figure, statistical significance was determined with the use of Student's t-test (A, C, D, E, F, H, I, J, K, and L). * $p<0.05$, ** $p<0.01$; n.s., not significant. See also Figure S1.

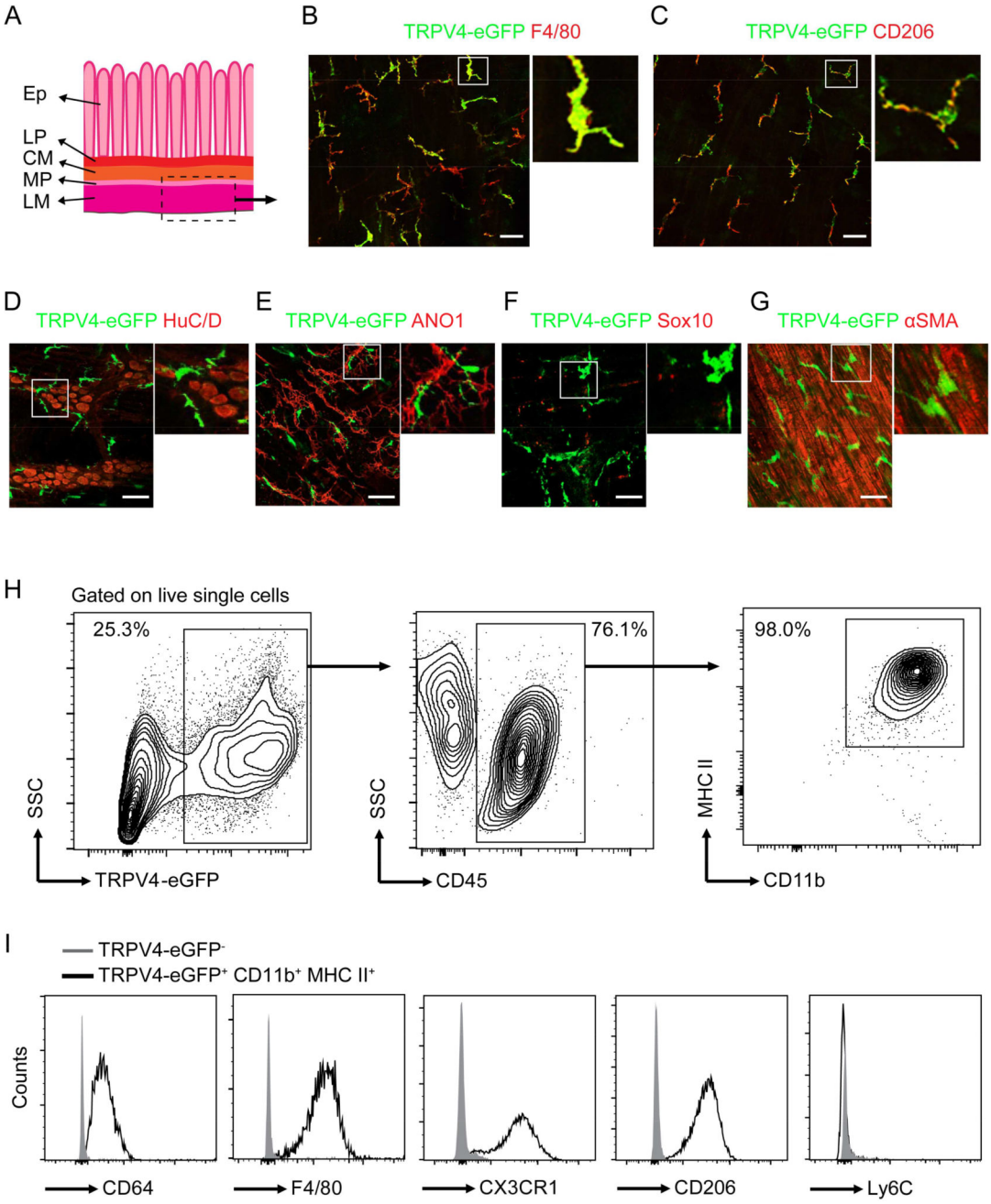

Figure 2. TRPV4 is selectively expressed by the colonic MMs

(A) Schematic diagram of whole-mount preparations of the longitudinal muscle layer and the myenteric plexus. Ep, epithelium; LP, lamina propria; CM, circular muscular layer; MP, myenteric plexus; LM, longitudinal muscular layer.

(B–C) Representative double immunofluorescent images of TRPV4-eGFP^{+} cells stained for F4/80 (B) and CD206 (C) in whole-mount preparations of the longitudinal muscle layer and myenteric plexus of the *Trpv4*^{eGFP} mice. Insets show digital-zoomed images of boxed areas. Scale bar=50 μm. One of three experiments is shown.

(D–G) Representative double immunofluorescent images of TRPV4-eGFP^{+} cells stained for HuC/D (D), ANO1 (E), Sox10 (F), or α-SMA (G) in whole-mount preparations of the longitudinal muscle layer and myenteric plexus of *Trpv4*^{eGFP} mice. Scale bar=50 μm. One of three experiments is shown.

(H) Flow cytometry analysis of TRPV4-eGFP^{+} cells for MM markers CD45, CD11b, and MHC II. One of three experiments is shown.

(I) Expression histograms of CD64, F4/80, CX3CR1, CD206, and Ly6C in TRPV4-eGFP^{-} and TRPV4-eGFP^{+} CD45^{+} cells. One of three experiments is shown.

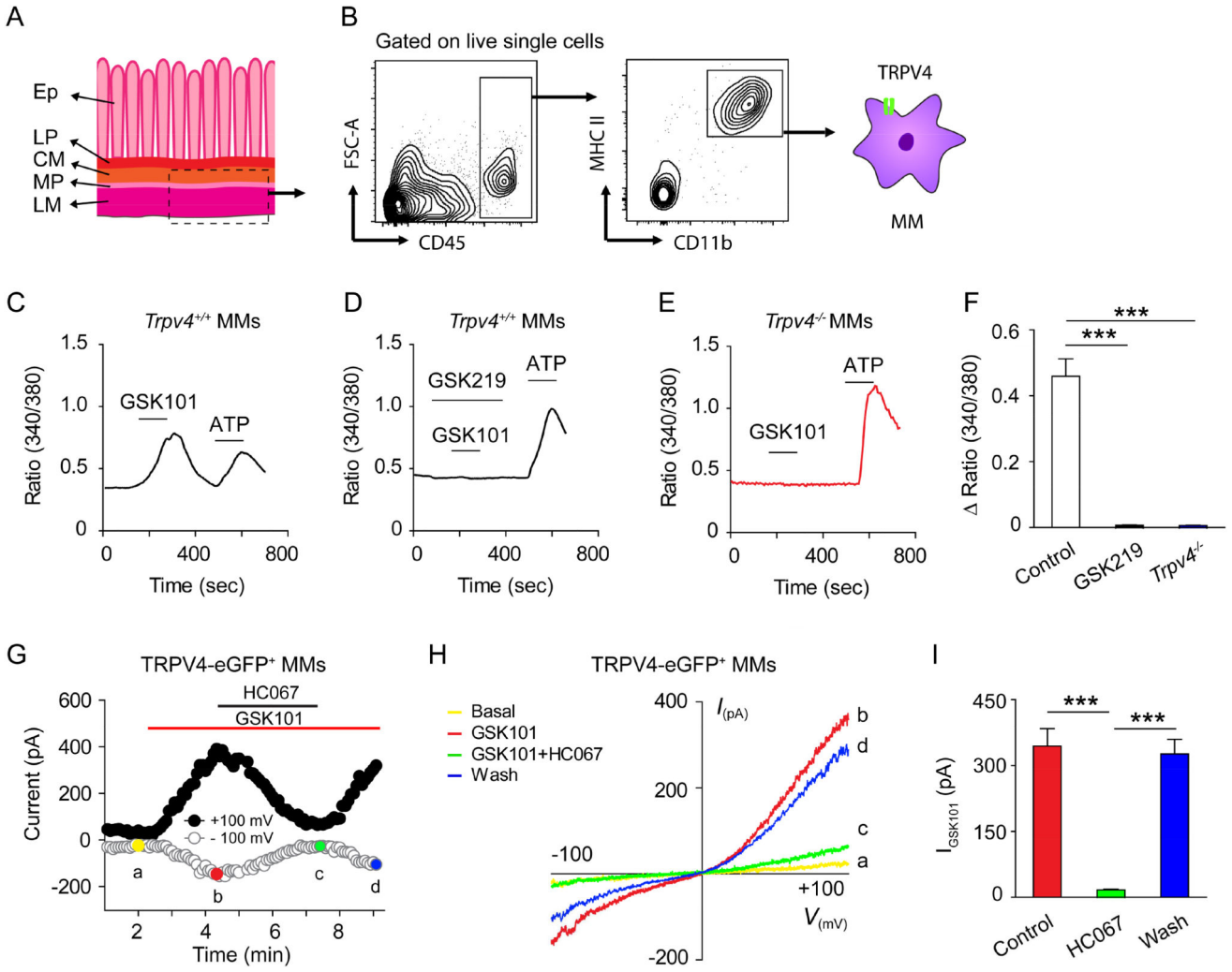

Figure 3. TRPV4 is functionally expressed by muscularis macrophages

(A) Schematic diagram of the colon tissue harvested for the isolation of MMs. Ep, epithelium; LP, lamina propria; CM, circular muscular layer; MP, myenteric plexus; LM, longitudinal muscular layer.

(B) Gating strategy for purifying $CD45^+$ $CD11b^+$ MHC II^+ MMs from the muscularis externa of mouse colon. One of five experiments is shown.

(C–F) Representative time-lapse Ca^{2+} imaging traces (C–E), and quantification (F) of GSK101-induced $[Ca^{2+}]_i$ response in sort-purified MMs from *Trpv4*$^{+/+}$ mice (C), MMs from *Trpv4*$^{+/+}$ mice exposed to the TRPV4 antagonist GSK219 (D), and MMs from the *Trpv4*$^{-/-}$ mice (E). ATP was used as a positive control. n=5 cover slips per group from two independent experiments.

(G) Time course of membrane currents evoked by GSK101 (0.3 μM) at +100 mV and −100 mV membrane potentials with and without co-application of the TRPV4 antagonist HC067. Horizontal bars denote the time courses for applications of GSK101 and HC067. One of three independent experiments is shown.

(H) Representative current-voltage curves taken at time points a, b, c, and d (color-coded) in (G). A ramp protocol elicited by a voltage ramp from −100 mV to +100 mV was used. One of three independent experiments is shown.

(I) Quantification of the effect of HC067 on GSK101-activated whole-cell membrane current recorded at +100 mV. n=6 cells per group from three independent experiments. Data are mean ± SEM. In this figure, statistical significance was determined using one-way ANOVA with Tukey's post hoc test (F and I). *** $p<0.001$. See also Figures S2–S3.

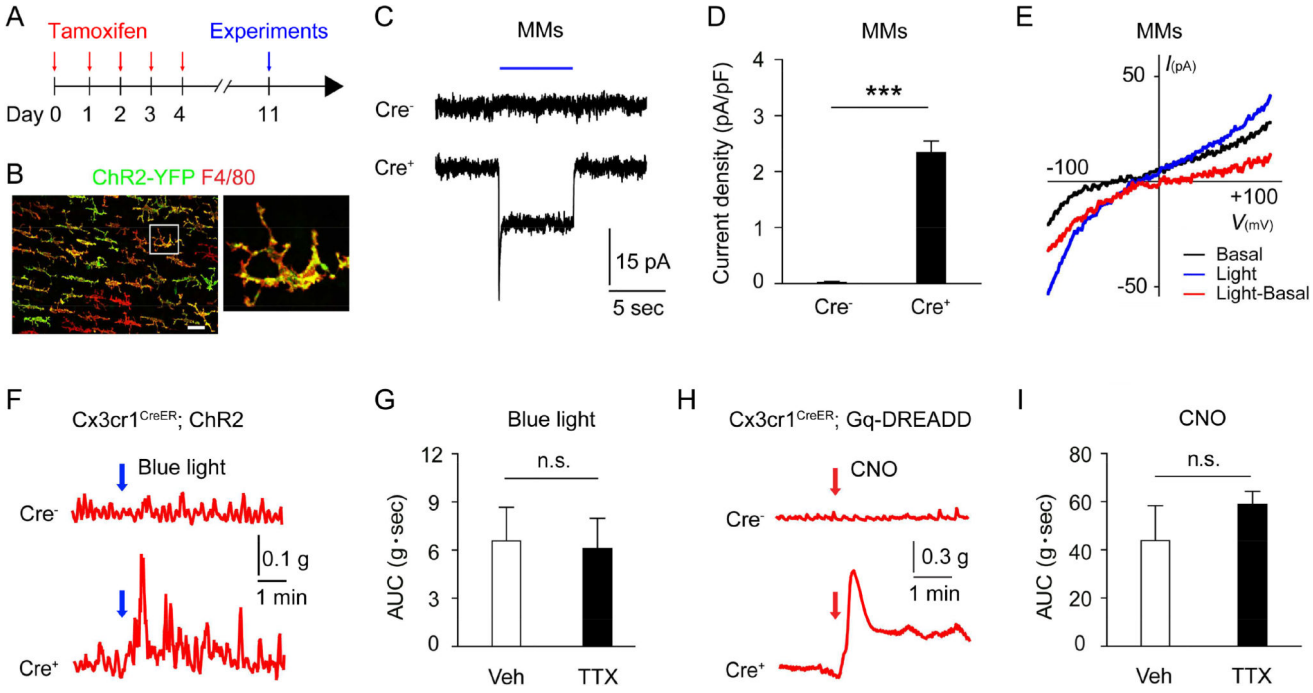

Figure 4. Selective stimulation of colonic macrophages produces ENS-independent colon contraction

(A) Schematic of Cre induction by tamoxifen administration.

(B) Representative immunofluorescent images of ChR2-YFP^{+} cells stained for F4/80 in the whole-mount preparations of the longitudinal muscle layer and the myenteric plexus from the colon of *Cx3cr1^{CreER};ChR2* mice. Scale bar=50 μm.

(C–D) Representative current traces (C) and quantification (D) of light-activated currents in sort-purified colonic MMs from Cre^{-} and Cre^{+} *Cx3cr1^{CreER};ChR2* mice.; n=12 cells in each group. Blue line represents the time of blue light illumination.

(E) Representative current traces of the I–V relationship of blue light-activated whole-cell membrane currents in response to voltage ramps from −100 mV to +100 mV. The red line represents the net ChR2-mediated current resulting from the subtraction of the blue light-evoked response (blue) by the basal response (black).

(F) Representative traces of light illumination (10 Hz, 20 ms pulse width)-induced colon contraction in Cre^{-} and Cre^{+} *Cx3cr1^{CreER}; ChR2* mice.

(G) Quantification of colon contraction induced by blue light illumination of the Cre^{+} *Cx3cr1^{CreER}; ChR2* mice in the presence of vehicle (0.1% DMSO) or TTX (0.3 μM). n=12 segments form 3 mice per group.

(H) Representative traces of CNO-induced colon contraction in Cre^{-} and Cre^{+} *Cx3cr1^{CreER};Gq-DREADD* mice.

(I) Quantification of CNO-induced colon contraction in Cre^{+} *Cx3cr1^{CreER};Gq-DREADD* mice in the presence of vehicle (0.1% DMSO) or TTX (0.3 μM). n=12 segments form 3 mice per group.

All data are pooled from two to three independent experiments. Data are mean ± SEM. In this figure, statistical significance was determined with the use of Student's t-test (D, G, and I). *** p<0.001; n.s., not significant.

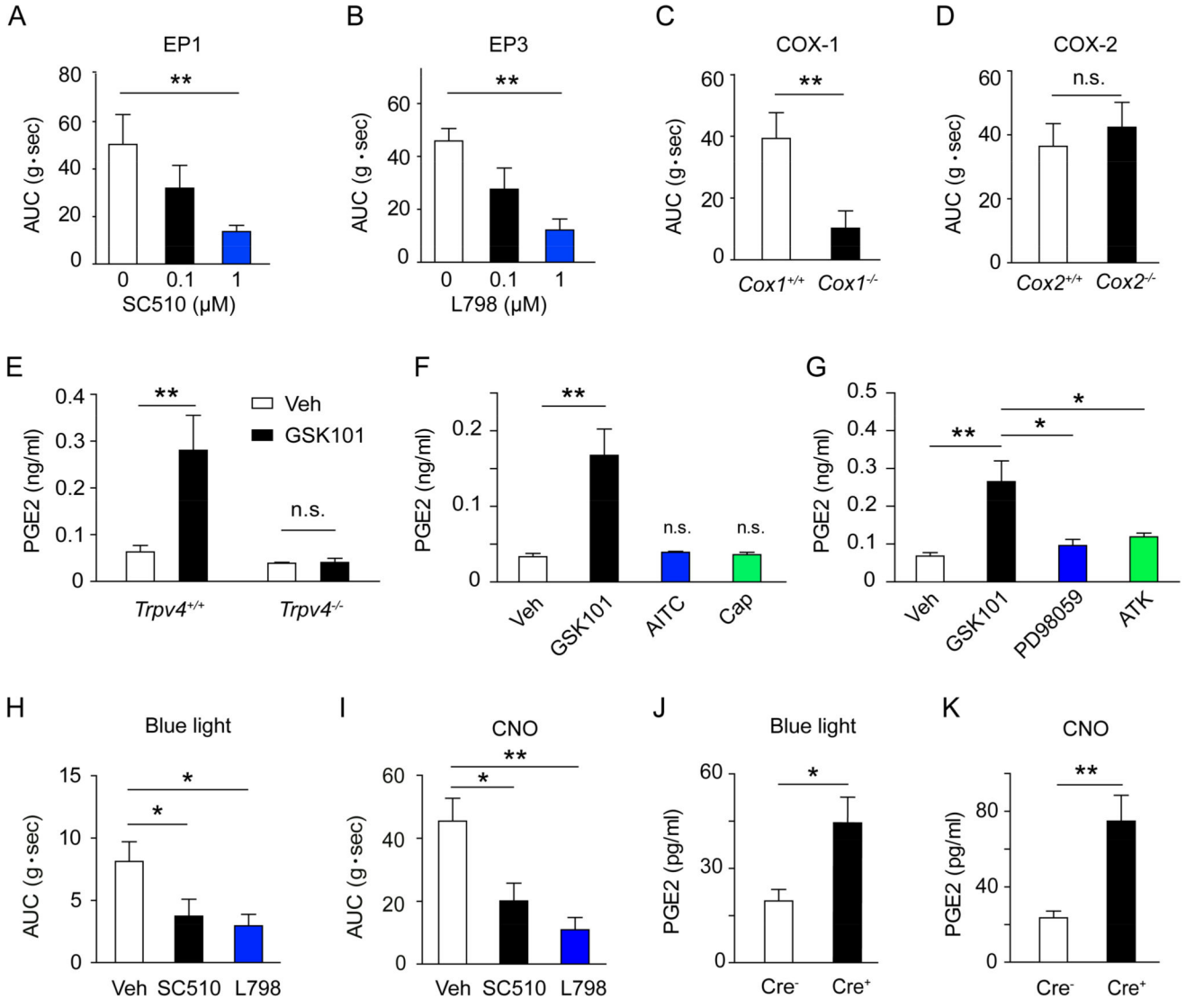

Figure 5. PGE2 signaling is critically involved in MM-mediated colon contraction

(A–B) Concentration-dependent inhibition of GSK101 (0.3 μM)-induced colon contraction by either the EP1 receptor antagonist SC510 (A) or the EP3 receptor antagonist L798 (B). n=16 segments from 4 mice per group.

(C–D) GSK101 (0.3 μM)-induced colon contraction in *Cox1*$^{-/-}$ (C) and *Cox2*$^{-/-}$ (D) mice and their *wt* controls. n=12 segments from 3 mice per group.

(E) PGE2 release from MMs sort-purified from *Trpv4*$^{+/+}$ or *Trpv4*$^{-/-}$ mice evoked by vehicle (0.1% DMSO) or GSK101 (0.3 μM). n=5 mice per group.

(F) PGE2 release from MMs evoked by vehicle (0.1% DMSO), GSK101 (0.3 μM), AITC (100 μM), or capsaicin (Cap, 0.5 μM). n=5 mice.

(G) Effects of the ERK1/2 inhibitor PD98059 (3 μM) or the PLA2 inhibitor ATK (10 μM) on GSK101 (0.3 μM)-induced PGE2 release from sort-purified MMs. n=5 mice per group.

(H) Quantification of colon contraction evoked by blue light illumination in Cre^{+} *Cx3cr1*^{CreER}*;ChR2* mice in the presence of vehicle (0.1% DMSO), the EP1 receptor

antagonist SC510 (1 uM), or the EP3 receptor antagonist L798 (1 uM). n=12 segments form 3 mice per group.

(I) Quantification of CNO-induced colon contraction in Cre^{+} *Cx3cr1^{CreER};Gq-DREADD* in the presence of vehicle (0.1% DMSO), the EP1 receptor antagonist SC510 (1 uM), or the EP3 receptor antagonist L798 (1 uM). n=12 segments form 3 mice per group.

(J–K) Quantification of PGE2 release from colonic MMs sort-purified from Cre^{-} and Cre^{+} *Cx3cr1^{CreER};ChR2* mice subjected to blue light illumination (J) or colonic MMs from Cre^{-} and Cre^{+} *Cx3cr1^{CreER};Gq-DREADD* mice subjected to CNO treatment (K). n=5 mice in each group.

All data are pooled from two to three independent experiments. Data are mean ± SEM. In this figure, statistical significance was determined using one-way ANOVA with Tukey's post-test (A, B, F, G, H, and I) and Student's t-test (C, D, E, J, and K).* $p<0.05$; ** $p<0.01$; n.s., not significant. See also Figure S4–S5

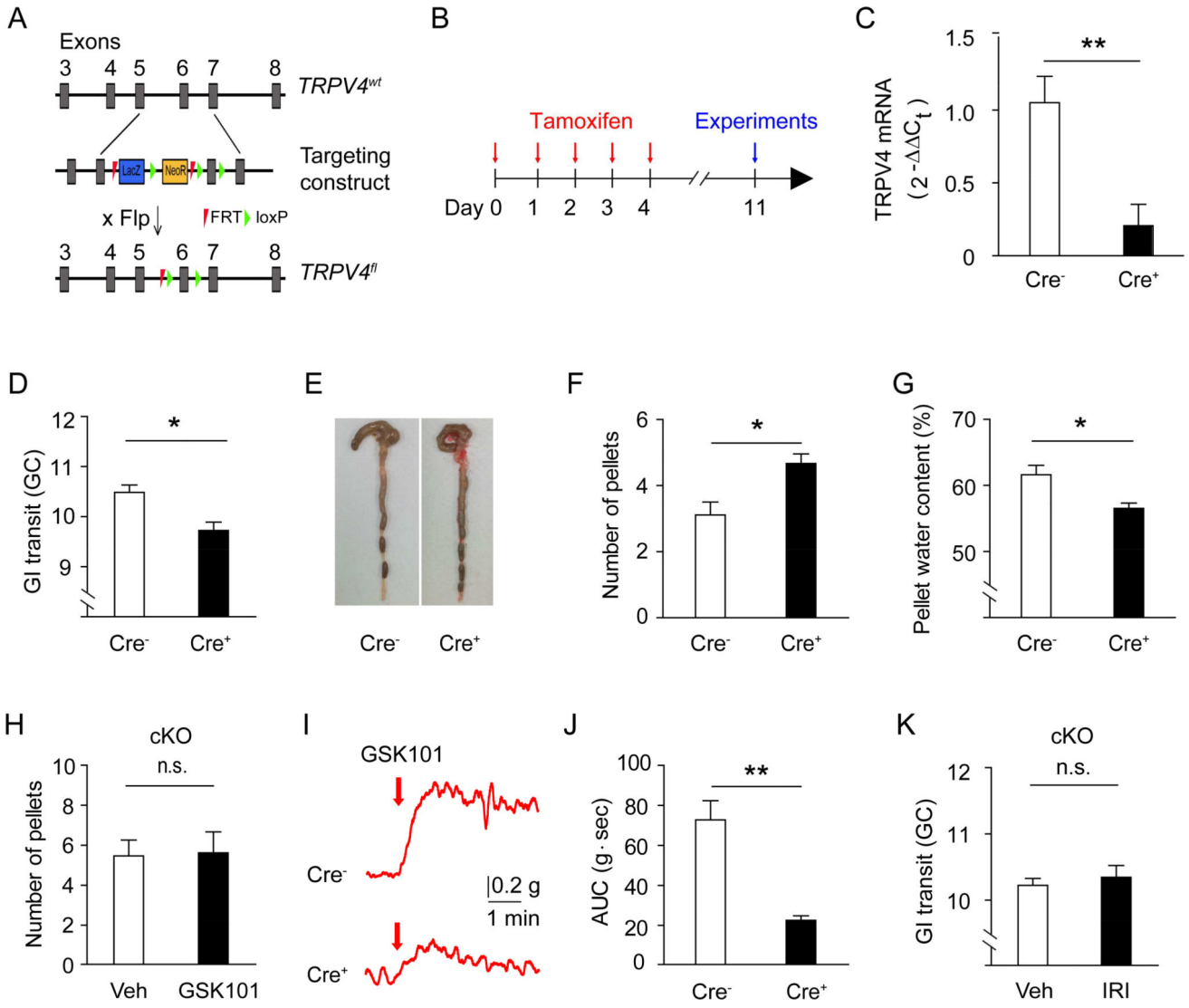

Figure 6. Macrophages-specific expression of TRPV4 controls gut motility in both homeostatic and pathological conditions

(A) Schematic for the generation of the *Trpv4*$^{f/f}$ allele. Flp, flippase recombinase.

(B) Schematic for the time course of Cre induction by tamoxifen administration.

(C) Quantitative analysis of TRPV4 levels by qRT-PCR in sort-purified colonic MMs of Cre^{+} *Cx3cr1*^{CreER}*;Trpv4*$^{f/f}$ mice compared to Cre^{-} littermates. n=6 mice per group.

(D) GI transit in Cre^{+} *Cx3cr1*^{CreER}*; Trpv4*$^{f/f}$ mice and Cre^{-} littermates. n=5 mice per group.

(E–F) Representative images (E) and quantification (F) of formed fecal pellets retained in the colon of Cre^{+} *Cx3cr1*^{CreER}*; Trpv4*$^{f/f}$ mice and Cre^{-} littermates. n=8 mice per group.

(G) Water content of fecal pellets of Cre^{+} *Cx3cr1*^{CreER}*; Trpv4*$^{f/f}$ mice and Cre^{-} littermates. n=9 mice per group.

(H) Total number of fecal pellets expelled within 30 min after i.p injections of vehicle (1% DMSO) or GSK101 (100 μg/kg) in Cre^{+} *Cx3cr1*^{CreER}*;Trpv4*$^{f/f}$ mice and Cre^{-} littermates. n=6 mice per group.

(I–J) Representative traces (I) and quantification (J) of GSK101 (0.3 μM)-induced colon contraction in Cre^{+} *Cx3cr1*^{CreER};*Trpv4*$^{f/f}$ mice and Cre^{-} littermates. n=12 segments from 3 mice per group.

(K) GI transit in Cre^{+} *Cx3cr1*^{CreER}; *Trpv4*$^{f/f}$ mice treated with vehicle (1% DMSO) or IRI (100 mg/kg). n=5 mice per group.

All data are pooled from two to three independent experiments. Data are mean ± SEM. In this figure, statistical significance was determined using Student's t-test (C, D, F, G, H, J, and K).* $p<0.05$; ** $p<0.01$; n.s., not significant.